SUPPORTING INFORMATION

Rational Design of 2D Ferroelectric Heterogeneous Catalysts for Controllable Hydrogen Evolution Reaction

Tsz Lok Wan[1#], Junxian Liu[1#], Xin Tan[2], Ting Liao[1], Yuantong Gu[1], Aijun Du[3], Sean Smith[2]*, Liangzhi Kou[1]*

[1] School of Mechanical, Medical and Process Engineering Faculty, Queensland University of Technology, Brisbane, QLD, Australia.

[2] Integrated Materials Design Laboratory, Department of Applied Mathematics, Research School of Physics, The Australian National University, Canberra, Australian Captial Territory, Australia.

[3] School of Chemistry and Physics, Queensland University of Technology, Brisbane, QLD, Australia.

# The authors made the equal contributions.

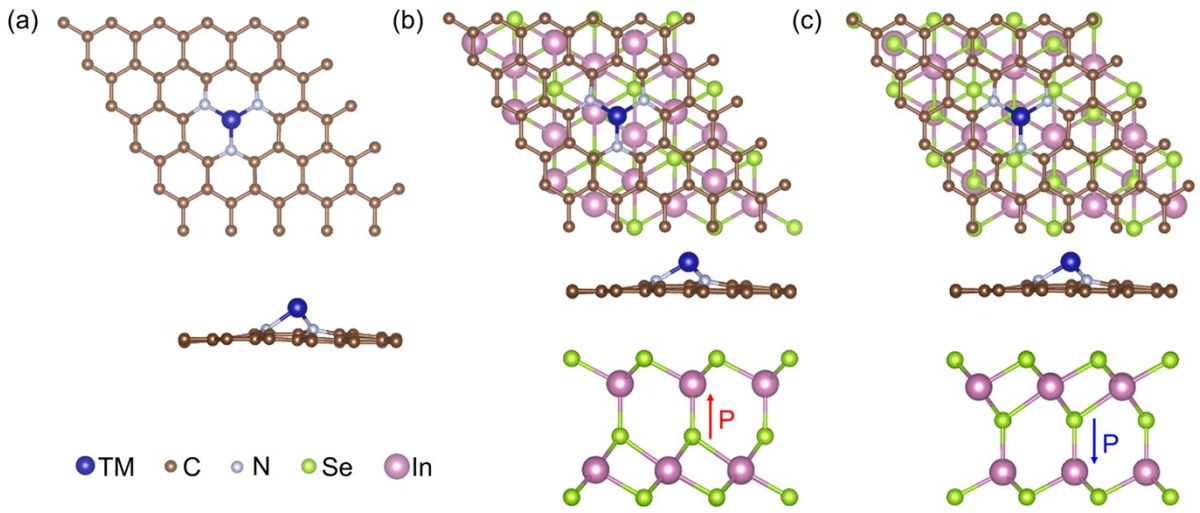

Fig. S1 Top and side views of the optimized structures for (a) TMN_3, (b) TMN_3/P↑-In_2Se_3, and (c) TMN_3/P↓-In_2Se_3.

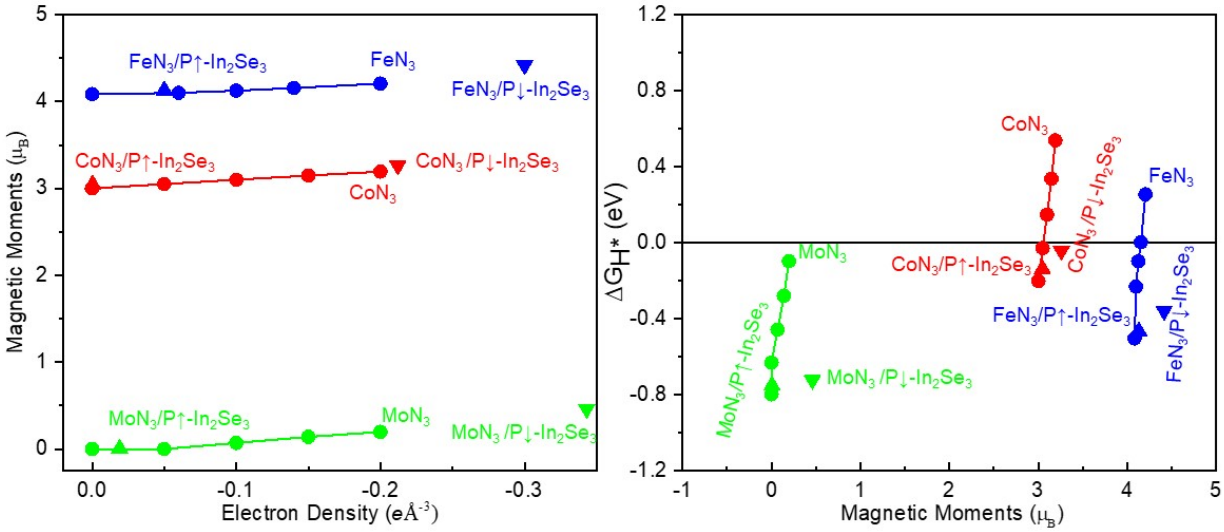

Fig. S2 Relationships between the (a) magnetic moment and electron density and (b) Gibbs free energy of ΔG_{H^*} and magnetic moment of TMN_3 and TMN_3/In_2Se_3 catalysts.

Fig. S2a shows the inverse relationship between the magnetic moment of TMN_3-H* and the different electron densities. It is found that the electron density can influence the magnetic moment of TMN_3-H*. On the other hand, the notable deviations from the linear trend between magnetic moment and electron density of TMN_3/P↑-In_2Se_3 and TMN_3/P↓-In_2Se_3 can be also observed. It can be attributed to the electrostatic potential difference after introducing the FE substrate and the intrinsic polarization of In_2Se_3, which is partially responsible for the variation of the magnetic moment. As shown in Fig. S2b, the larger magnetic moment adjusts the catalytic activity of TM sites, resulting in weaker adsorption of the H atom on the TMN_3

catalyst, ascribed to the adjustment of empty and occupied d-orbitals of TM atoms. Further analysis can be seen in Fig. 1c-e, 2b, and S4.

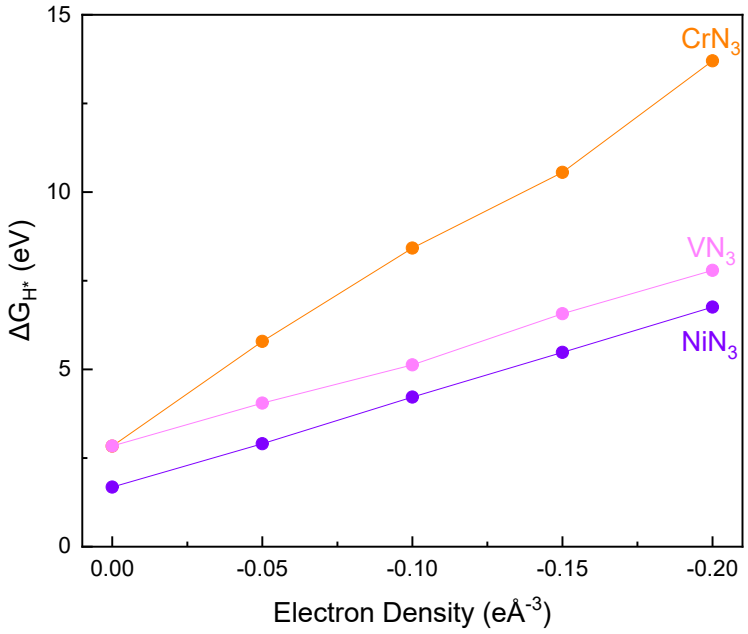

Fig. S3 Relationships between the Gibbs free energy of ΔG_{H^*} and electron density of other TMN_3 catalysts.

One can see clearly from Fig. S3 that a linear relationship between the electron density and ΔG_{H^*} for other studied TMN_3 catalysts (TM = Cr, Ni, and V), indicates electron density is an effective factor to modulate the HER performance. However, these three TMN_3 catalysts show weak HER activity, thus, we neglect these TMN_3 catalysts in the following discussion.

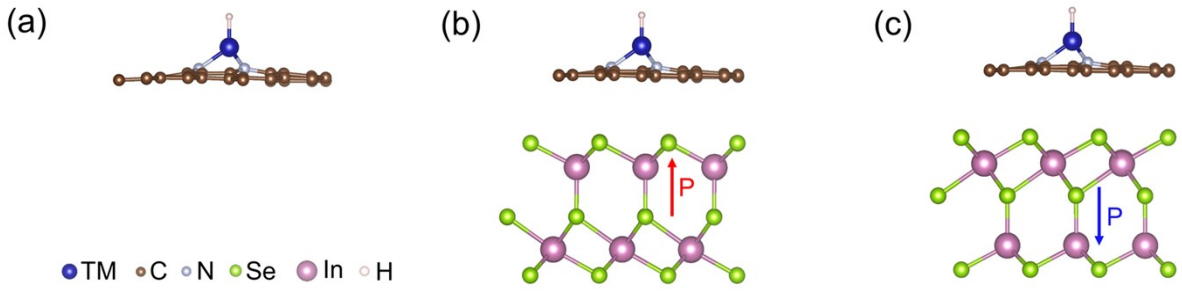

Fig. S4 Side views of the optimized structures for (a) TMN_3-H*, (b) TMN_3/P↑-In_2Se_3-H*, and (c) TMN_3/P↓-In_2Se_3-H*.

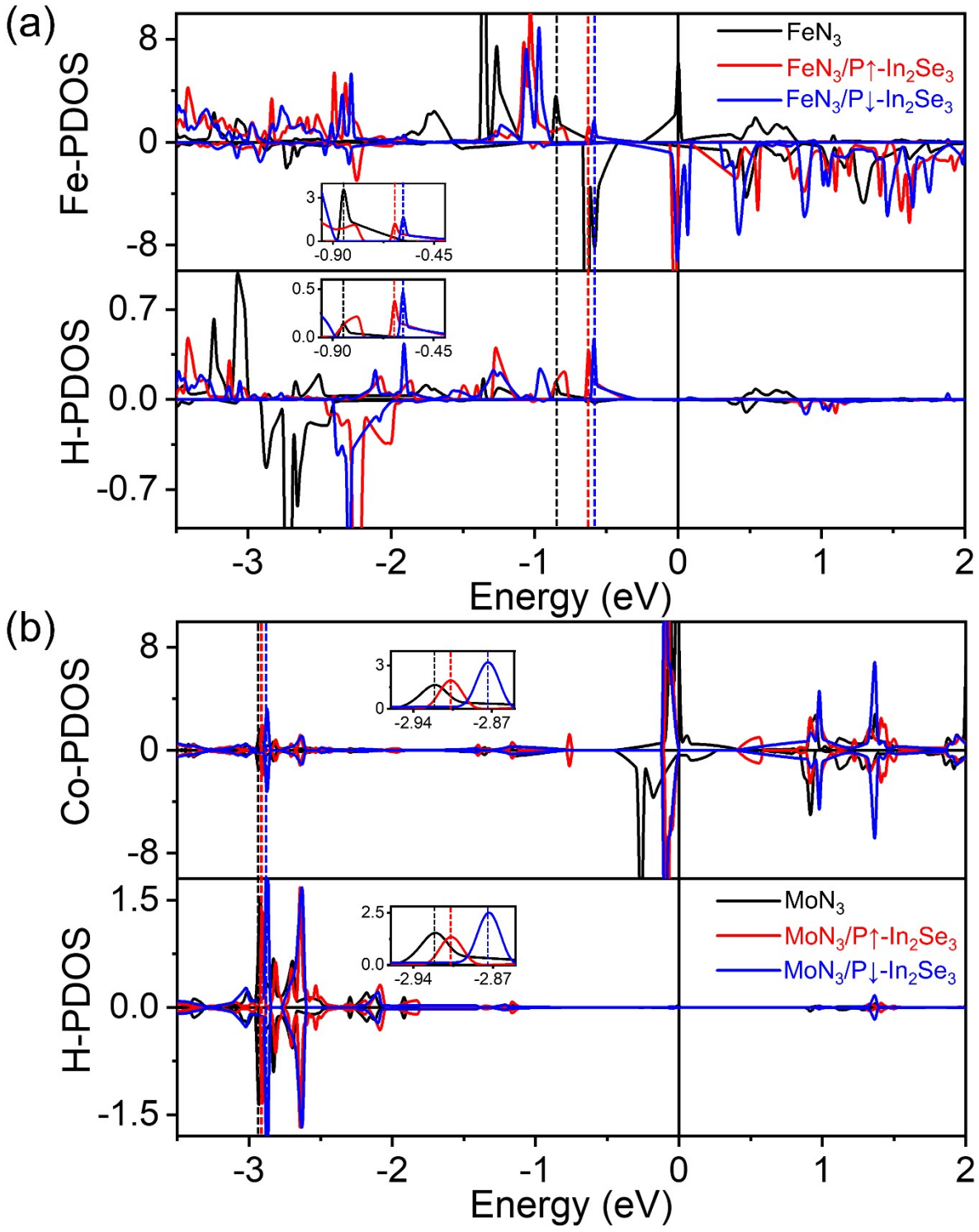

Fig. S5 PDOSs of TM-d and H-s orbitals for TMN_3 and TMN_3/In_2Se_3 with different polarization directions: (a) FeN_3 and (b) MoN_3.

From Fig. S5, we can see the PDOS for Fe/Mo-d and H-s orbitals of pure TMN_3 and TMN_3/In_2Se_3 are plotted in Fig. S4. One we can see the obvious shift of Fe/Mo–H bonding state when Fe/MoN_3 is placed on the In_2Se_3 with two different polarization directions, and it agrees with the changes of ΔG_{H^*} values.

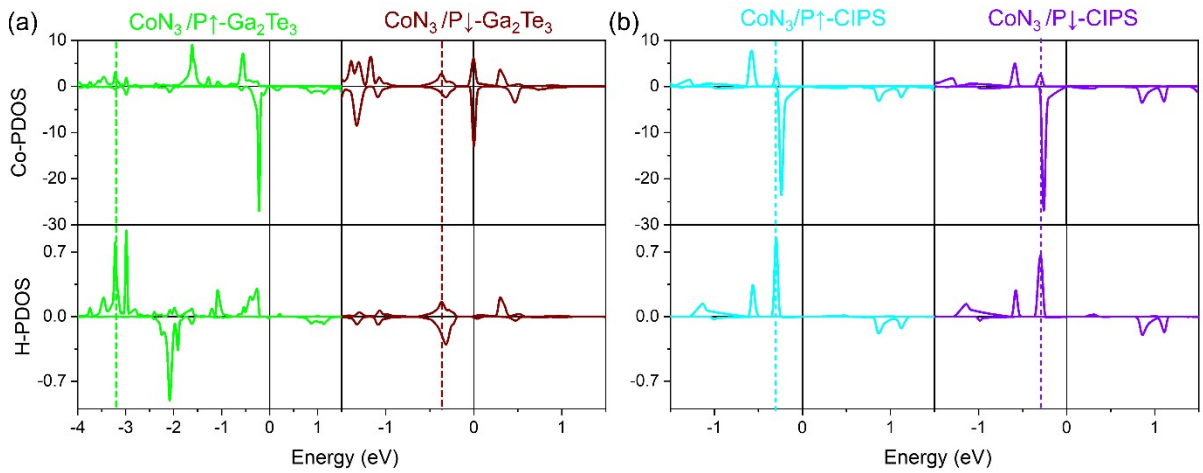

Fig. S6 PDOSs plot for (a) CoN_3/Ga_2Te_3 and (b) CoN_3/CIPS with different polarization directions.

Fig. S6 shows the PDOS for Co-d and H-s orbitals of CoN_3/Ga_2Te_3 and CoN_3/CIPS with two different polarization directions. In Fig S6a, when Co/MoN_3 is placed on the P↑-Ga_2Te_3, the overlap between the Co-d and H-s orbitals is located at the deep level, demonstrating the relatively high bonding interaction between the Co and H atoms. In contrast, the hybridization between the Co-d and H-s orbitals moves towards the Fermi level when the polarization direction of Ga_2Te_3 points down, indicating the weak chemical binding of Co-H bond.

As provided in Fig. S6b, one can see clearly that the PDOS of Co-d and H-s orbitals remains essentially unchanged in both polarization directions of CIPS, leading to the feeble changes of the magnetic moment and electron transfer. The phenomenon can be attributed to CIPS is a layered ferroelectric which has a relatively weak van der Waals interaction between the catalyst/substrate interface, leading to a weak response to the polarization switching.

Table S1. The H adsorptions on the pure TMN_3 and TMN_3/In_2Se_3: Gibbs free energy change of H* intermediate (ΔG_{H^*} in eV), total magnetic moment of TMN_3 (M in μ_B), electron transfer of TM atoms (Q_{TM} in *e*/atom), N atoms (Q_N in *e*/unit cell), In_2Se_3 substrate ($Q_{In_2Se_3}$ in *e*/unit cell), and H atoms (Q_H in *e*/atom).

System	ΔG_{H^*}	M	Q_{TM}	Q_N	$Q_{In_2Se_3}$	Q_H
FeN_3	-0.504	4.08	-1.09	3.68	N/A	0.45
FeN_3/P↑-In_2Se_3	-0.465	4.13	-1.09	3.69	0.05	0.44
FeN_3/P↓-In_2Se_3	-0.360	4.42	-1.13	3.719	0.30	0.41
MoN_3	-0.798	0.00	-1.43	3.459	N/A	0.45
MoN_3/P↑-In_2Se_3	-0.751	0.00	-1.43	3.46	0.02	0.43
MoN_3/P↓-In_2Se_3	-0.723	0.46	-1.42	3.48	0.34	0.43

Table S2. Gibbs free energy change of H* intermediate (ΔG_{H^*} in eV) for pure TMN_3.

System	ΔG_{H^*}
CrN_3	2.836
NiN_3	1.680
VN_3	2.840

Table S3. The magnetic moment of the catalytic TM sites and the surrounding atoms under the different electron doping.

Electron Doping	CoN_3					FeN_3					MoN_3				
	Co	N	C	H	Total	Fe	N	C	H	Total	Mo	N	C	H	Total
0	2.30	0.09	0.01	0.02	3.00	3.44	0.08	0.01	0.00	4.08	0.00	0.00	0.00	0.00	0.00
-0.05	2.31	0.10	0.01	0.02	3.05	3.49	0.08	0.01	0.00	4.10	0.00	0.00	0.00	0.00	0.00
-0.1	2.33	0.10	0.01	0.02	3.10	3.49	0.08	0.01	0.00	4.13	0.11	0.00	0.00	0.00	0.07
-0.15	2.34	0.10	0.01	0.02	3.15	3.50	0.09	0.01	0.00	4.16	0.22	0.01	0.00	0.00	0.14
-0.2	2.36	0.10	0.01	0.02	3.19	3.51	0.09	0.00	0.00	4.21	0.31	0.01	0.00	0.00	0.20

Table S4. The magnetic moment of the catalytic TM sites and the surrounding atoms before and after absorbed H atom. The values in brackets denote the magnetic moment after absorbed H atom.

System		TMN_3	$TMN_3/P\uparrow$-In_2Se_3	$TMN_3/P\downarrow$-In_2Se_3
Co	Co	1.90	1.94	2.00
		(2.30)	(2.30)	(2.30)
	N	0.07	0.07	0.09
		(0.09)	(0.09)	(0.10)
	C	0.01	0.00	0.00
		(0.01)	(0.01)	(0.00)
	H	N/A	N/A	N/A
		(0.02)	(0.02)	(0.02)
	Total	2.29	2.33	2.49
		(3.00)	(3.01)	(3.26)
Fe	Fe	3.01	3.04	3.08
		(3.44)	(3.48)	(3.49)
	N	0.05	0.06	0.07
		(0.08)	(0.09)	(0.09)
	C	0.01	0.00	0.00
		(0.01)	(0.01)	(0.00)
	H	N/A	N/A	N/A
		(0.00)	(0.00)	(0.00)
	Total	3.19	3.27	3.50
		(4.08)	(4.13)	(4.42)
Mo	Mo	1.18	1.32	1.54
		(0.00)	(0.00)	(0.29)
	N	0.02	0.02	0.02
		(0.00)	(0.00)	(0.01)
	C	0.01	0.00	0.00
		(0.00)	(0.00)	(0.00)
	H	N/A	N/A	N/A
		(0.00)	(0.00)	(0.00)
	Total	1.02	1.13	1.53

	(0.00)	(0.00)	(0.46)